Single-cell mass spectrometry reveals the importance of genetic diversity and plasticity for phenotypic variation in nitrogen limited *Chlamydomonas*

Jasmin Krismer[1], Manu Tamminen[2,3], Simone Fontana[2], Renato Zenobi[1*], Anita Narwani[2*]

Affiliations

[1] Department of Chemistry and Applied Biosciences (D-CHAB), ETH Zurich, Zurich, Switzerland

[2] Eawag, Swiss Federal Institute of Aquatic Science and Technology, Dubendorf, Switzerland

[3] Department of Environmental Systems Science, ETH Zurich, Switzerland

Correspondence:

Renato Zenobi, Institute for Chemistry and Applied Biosciences, Vladimir-Prelog-Weg 3, 8093 Zürich, Switzerland.

Tel.: +41 44 632 43 76

Fax : +41 44 632 12 92

E-mail: zenobi@org.chem.ethz.ch

Anita Narwani, BU-G11 Überlandstrasse 133, Department of Aquatic Ecology, Eawag (Swiss Federal Institute of Aquatic Science and Technology), 8600 Dübendorf, Switzerland

Tel.: +41 58 765 5667

Fax : +41 58 765 5802

E-mail: anita.narwani@eawag.ch

This document is the accepted manuscript version of the following article: Krismer, J., Tamminen, M., Fontana, S., Zenobi, R., & Narwani, A. (2017). Single-cell mass spectrometry reveals the importance of genetic diversity and plasticity for phenotypic variation in nitrogen-limited Chlamydomonas. ISME Journal, 11(4), 988-998. https://doi.org/10.1038/ismej.2016.167

Support: J.K. and M.T. are funded directly by ETH

Conflict of interest: The Authors declare no conflict of interest.

Subject category: Integrated genomics and post-genomics approaches in microbial ecology

Abstract

Phenotypic variation is vital for microbial populations to survive environmental perturbations. Both genetic and non-genetic factors contribute to an organism's phenotypic variation and therefore its fitness. To investigate the correlation between genetic diversity and phenotypic variation, we applied our recently developed mass spectrometry method that allows for the simultaneous measurement of more than 25 different lipids and pigments with high throughput in the unicellular microalga *Chlamydomonas reinhardtii*. We monitored the impact of nitrogen limitation on a genetically diverse wild-type strain CC-1690 and two isoclonal isolates from CC-1690 named ANC3 and ANC5. Measuring molecular composition of thousands of single cells at different time points of the experiment allowed us to capture a dynamic picture of the phenotypic composition and adaptation of the populations over time. While the genetically diverse population maintained phenotypic variation over the whole time course of the experiment, the isoclonal cultures showed higher synchronicity in their phenotypic response. Furthermore, the genetically diverse population showed equal or greater phenotypic variation over the whole time range in multidimensional trait space compared with isoclonal populations. However, along individual trait axes non-genetic variance was higher in isoclonal populations.

Introduction

The ability of organisms to express phenotypic variation is a basic feature of life. The expression of phenotypic variation among individuals within a population can increase the chances that some individuals in a population will express adaptive phenotypes in a new or changed environment (Forsman and Wennersten, 2016), and therefore improve the fitness of the species, and increase the chances of its survival (reviewed in Schlichting and Pigliucci, 1998). Phenotypic variation of organisms can result from genomic differences among individuals, but may also occur in isogenic populations due to phenotypic plasticity, epigenetic effects, and bet-hedging, among others (Ackermann, 2015, Simons, 2011, Wennersten and Forsman, 2012). Understanding the relative contributions of genetic and non-genetic sources of phenotypic variation is particularly important in studies of evolution and eco-evolutionary feedbacks for numerous reasons (Ghalambor et al., 2007, Pigliucci, 2005, DeWitt et al., 1998, Auld et al., 2010, Simons, 2011, Hairston et al., 2005, Collins and Gardner, 2009, Yamamichi et al., 2011, Hendry, 2016). First, plasticity and other non-genetic sources of variation may be more limited in the extent of phenotypic variation that can generate than genetic sources of variation (Gienapp et al., 2008, DeWitt et al., 1998, Auld et al., 2010). Second, genetic and non-genetic phenotypic variation respond to environmental change at different rates, with the expectation that non-genetic sources of variation tend to respond faster (Yamamichi et al., 2011). Lastly, due to the first two points above, the relative contributions of each may differ depending on the rate and strength of environmental change observed (Yamamichi et al., 2011, Hendry, 2016). Furthermore, in order to predict evolutionary responses of populations to future environments, an estimate of the genetic basis of phenotypic variance among individuals is required (Schlichting and Pigliucci, 1998). In this paper we provide the first comparison of the extent to which genetic and non-genetic

68 mechanisms are capable of producing phenotypic variation in a well-studied alga
69 (*Chlamydomonas reinhardtii*) under a well-studied stress (nitrogen limitation) at the level of
70 the single cell.

71 While there is a wealth of recently developed methods for extracting single-cell
72 information from genomes (Lu et al., 2012, Zong et al., 2012), transcription (Macosko et al.,
73 2015, Klein et al., 2015) and protein expression (Spitzer and Nolan, 2016), methods for the
74 multiparametric analysis of metabolites in single cells are scarce (Zenobi, 2013). What is
75 more, the great majority of these techniques were developed for mammalian cells. Some
76 methods with single-cell sensitivity have successfully been transferred to microbes, including
77 genome analysis (Kashtan et al., 2014, Rinke et al., 2013, Spencer et al., 2016) and the
78 characterization of phenotypes using fluorescence (Breker et al., 2013, Fontana et al., 2014),
79 Raman microscopy (Schuster et al., 2000) or elemental analysis of isotopes using secondary
80 ion mass spectrometry (Schreiber et al., 2016). However, in general, applying single-cell
81 methods to microbes is challenging due to the great diversity of cell sizes, morphologies and
82 structural properties of cell walls. Therefore, the study of phenotypic variation in microbial
83 systems and its underlying mechanisms is still compromised by technical limitations in
84 microbial systems (Altschuler and Wu, 2010, Ackermann, 2015).

85 We recently developed a method for the label-free analysis of small molecules in
86 single cells of the microalga *Chlamydomonas reinhardtii*, which combines matrix-assisted
87 laser desorption/ionization (MALDI) mass spectrometry (MS) with high-throughput
88 microarray sample-preparation technology. This technique, here called single-cell mass
89 spectrometry (SC-MS), showed the reproducible relative quantitative measurements of more
90 than 15 lipids and pigments in thousands of single cells of a unicellular organism for the very
91 first time (Krismer et al., 2015). *Chlamydomonas reinhardtii* is a popular model organism in

laboratory evolution experiments owing to the tools developed for transformation and sequencing of the genome (Merchant et al., 2007). Abiotic stress in *C. reinhardtii* is often linked with light availability, or macronutrient limitation. Phosphorous and nitrogen are among the most limiting macronutrients (Reynolds, 2006). Metabolic adaptations to nitrogen limitation are well characterized in *C. reinhardtii* and are the subject of continued study (Park et al., 2015). The main metabolic adaptations to nitrogen limitation include the downregulation of photosynthetic activity (Juergens et al., 2015, Huner et al., 2012), the accumulation of lipid droplets, and the increased mobilization and allocation of internal and external nitrogen (Miller et al., 2010). The downregulation of photosynthesis (reflected by fewer photosynthetic pigments such as chlorophyll-a) and the accumulation of neutral lipids (consisting mainly of triacylglycerols, hereafter "TAG"s) are attributed to a decreased utilization of reductant energy due to a slowdown in anabolic metabolism (Huner et al., 2012). Different strains of *C. reinhardtii* do however display marked phenotypic differences in their responses to N-limitation (Siaut et al., 2011). In a recent study, Malcom and coworkers investigated the genetic basis of growth rate variation across 18 strains of *C. reinhardtii* across 30 environments and found that, while genetically-based phenotypic variation was constrained to only three main axes of selection (types of environmental variation), the response to nitrogen availability was one of them (Malcom et al., 2015) .

Here, we extended our SC-MS method to measure the impact of genetic diversity and plasticity (here defined as all phenotypic variation expressed by isoclonal populations including phenotypic heterogeneity (Ackermann, 2015)) in generating phenotypic variation under nitrogen-limited conditions. SC-MS was able to detect 26 small molecules from different pigment and lipid classes in individual cells, including chlorophylls, thylakoid lipids, membrane lipids and storage lipids (**Table 1**). Here we measured the lipid composition of

thousands of single cells to determine the variance and the composition of phenotypes present in different populations over time. We further investigated the correspondence between measures of population-level growth, resource limitation and single-cell phenotypes to investigate the possibility of different strategies in dealing with nitrogen limitation. To do so, we cultured the genetically diverse strain CC-1690 and two isoclonal populations isolated from CC-1690 termed ANC3 and ANC5 under N-replete and N-deplete conditions for 9 days. Population-level characterization showed differences among the populations selected for this experiment in their growth rate (μ_{max}, Figure S1) and in their minimum nitrogen requirements (referred to here as R*, Figure S1). By sampling multiple time points of batch growth for SC-MS, we captured the adaptation to nitrogen depletion in the different cultures with single-cell resolution.

Materials and methods

Microbial populations and culture conditions

CC-1690 wild type mt+ was obtained from the Chlamydomonas Resource Center, University of Minnesota (http://www.chlamycollection.org). The culture inoculum was grown up in sterile COMBO freshwater medium (Kilham et al., 1998) lacking silicate, animal trace elements and vitamins, and then again plated onto YA agar plates in order to allow for the formation of individual isoclonal colonies. Five isoclonal isolates were selected from agar plates by haphazardly picking five spatially isolated and distinguishable colonies and inoculating them again into liquid medium. These isoclonal isolates were designated as Ancestors 1-5 (ANC1-ANC5).

Prior to the single-cell MS experiment, we performed an extensive set of pilot experiments to determine the population-level growth trajectories, growth rates and minimum rates of each population in media containing a wide range of nitrate concentrations (see detailed methods in the Supplementary information, Section 3.1). Based on these data (Figures S1-S3), we selected ANC3 and ANC5 for further investigation at the single-cell level because they showed distinct population-level characteristics relative to each other and to their parental population, CC1690. In particular, ANC3 showed a high growth rate (μmax_{ANC3} = 0.96 d^{-1}) and a higher nitrogen requirement (R^*_{ANC3} =1.78 µM N) than CC-1690($\mu max_{CC\text{-}1690}$ = 0.80 d^{-1} ,$R^*_{CC\text{-}1690}$ = 0.27 µM N). ANC5 showed a lower growth rate (μmax_{ANC5} = 0.54 d^{-1}) than CC-1690 and a nitrogen requirement of R^*_{ANC5} = 0.5 µM N.

Nitrate limitation experiments

Before performing the single-cell MS experiments, the wild type strain CC-1690 and the two isoclonal isolates, ANC3 and ANC5, were acclimated and inoculated as described in

Supplementary information, Section 3.2. The batch-cultures were maintained at 20 °C, at a light intensity of *ca.* 100 µEinstein m^{-2} s^{-2}, and under 100 rpm continuous shaking for nine days. We stopped the single-cell experiment on day 9 because growth trajectories from the pilot experiments had shown that the deplete cultures had all reached steady-state after 8 days, at which time the replete cultures were also approaching steady-state (Figure S3). For SC-MS, the cultures were sampled 2, 4, 6 and 9 days after inoculation. We sampled the cultures for dissolved nitrogen and phosphorus and for microscopy and on days 2 and 9 (details in the Supplementary information, Section 3.3 and 3.4). The dissolved nutrient samples showed that the nitrogen concentrations were always below the 0.25 mg L^{-1} detection limit in the deplete medium, and that the concentrations of nitrogen had decreased over time in the replete environment (Table S1).

Single-cell mass spectrometry

Single-cell MALDI mass spectrometry was performed as described recently (Krismer et al., 2015). In short, slides were prepared for SC-MS as follows: on each day each culture covered a complete stainless steel slide (of 1430 spots each). Each spot was 300 µm in diameter and had a center-to-center distance of 720 µm. A layer of matrix, corresponding to approx. 5 nl of a 10mg/ml solution of 2, 5-DHB (Sigma Aldrich, 85707) in 80% aqueous acetone, was deposited before spotting the cells. Cells were centrifuged three times at 5'000 g for 5 min and re-suspended in deionized water. The integrity of the cells was monitored by fluorescence microscopy throughout the sample preparation as shown in previously published work (Krismer et al., 2015). To adjust the number of cells per spot for increased single-cell yield on the target the optimal number of drops was determined for each culture using a dilution series (4x4 array of 1, 2, 3, 5, 10 drops of cell solution). The rest of the slide was covered with cells and the cells were quenched immediately using liquid nitrogen. The slide

was reconstituted to room temperature in a desiccator and lipids were extracted from the cells and co-crystallized with the MALDI matrix. The extraction was performed in five consecutive cycles (each approx. 5 nl of 10 mg/ml DHB in 80% aqueous acetone) for homogeneous lipid extraction. The whole procedure was monitored using a confocal fluorescence scanner (LS400, Tecan, Switzerland). The number of cells per spot was determined based on a confocal scan of the slides after quenching with liquid nitrogen. MALDI-MS parameters for the measurements on the MALDI TOF-TOF mass spectrometer (AB Sciex 5800, Sciex, Canada) were as follows: the laser was operated at a repetition rate of 400 Hz and an intensity of 4300-4400 arbitrary units. Spectra were measured for the range of 550-1000 m/z with an extraction delay time of 200 ns, exhaustively ablating each spot using a spiral pattern. The absence of MS and fluorescence signals in empty spots ensures that there is no cross-contamination, and spots with multiple cells were discarded before data analysis. Details on spectral processing and peak assignment of the mass spectra can be found in the Supplementary information, Section 3.5 and 3.6. A table of with peak assignments can be found in Table S2. A more detailed description of the SC-MS method can be found in (Krismer et al., 2015). Due to technical problems during the spotting only very few single cells of ANC5 culture were successfully measured on days 4 and 6.

Data analysis for single-cell mass spectrometry

A principal component analysis (PCA) on the dataset, including all populations, all nitrogen conditions and all days of the time series, was performed (princomp in R 3.2.4 Revised). A detailed procedure for the handling of the data (including spectral processing), submitted to PCA analysis can be found in Figure S7. The recorded peak areas span three orders of magnitude thus the dataset was square root transformed. We used ggplot2 function including the contour plot tool density2d for visualization of the PCA (Wickham, 2009). The

198 first five principal components (PC) explain 91.8 % of the observed variance in the dataset
199 (see Figure S8). The PC1 (49.5 % of variance explained) shows all-negative signs. The fact
200 that all PC loadings have the same sign indicates that this PC does not refer to relative but to
201 absolute intensities, which is underlined by the fact that the loadings closely resemble the
202 average intensity of the peak in the experiment (see Figure S9). In MALDI mass spectra, only
203 relative abundances hold quantitative information thus we restricted our interpretation on the
204 other PC's showing loadings with opposite signs. This is especially relevant in single-cell
205 analysis, since there is no option for introducing an internal standard and there is no single
206 compound that is present in equal amounts in each cell. The PC2 explains 26.0 % of the
207 observed variance and segregates between photosynthetic pigments and the extra-plastidic
208 Diacylglyceryltrimethylhomo-Ser lipids (hereafter "DGTS", Supplementary Information,
209 Figure S9). PC3 explains 8.2 % of the observed variance and segregates cells that detect high
210 levels of TAG storage lipids. PC4 explains 4.2 % of the observed variance and segregates
211 between DGTS lipids of different fatty acid composition. Details on non-parametric testing
212 can be found in Supplementary Material, Section 3.7.

213 Based on plots of cellular phenotypes on PC2 and PC3, we assigned cells to one of
214 three apparent phenotypic categories. Based on the cut-offs of the PC scores, we defined three
215 categorical phenotypes as 'high chlorophyll' (PC3 < 5, PC2 > 0), 'high membrane lipid' (PC3
216 < 5, PC2 < 0) and 'high storage lipid' (PC3 > 5). The absolute numbers of cells in each
217 phenotypic class can be found in Table S3. Contingency table analysis of Table S3 by means
218 of the Fisher's exact test was performed using Myfisher23.m function (Cardillo, 2007).
219 Details on the bivariate data analysis can be found in the Supplementary Material, Section
220 3.8.

221 In order to compare the whole range of phenotypic variation observed in the isoclonal

populations to that observed in the genetically diverse population, we calculated an index of multidimensional individual-level trait variation, called "Trait Onion Peeling" or TOP (see Fontana et al., 2016 for detailed description and methods). For this analysis we were interested in the total amount of multidimensional phenotypic space covered by a population in a given treatment over the course of the whole experiment, and so we pooled all of the cells in each population x nutrient combination over time. In order to compare samples of equal size for each treatment, we performed a bootstrap resampling of 100 cells from each population x nutrient combination 1000 times and calculated the TOP index on the PC2 and PC3 scores of the cells in each sample. We then compared the TOP index for each bootstrapped isoclonal population to the TOP index of a bootstrapped CC1690 population, and using the 1000 repeated bootstraps, we calculated the probability that a difference in trait variation between the isoclonal populations and the genetically diverse was greater than or less than zero.

Results

Phenotypic differences among populations and treatments over time

To characterize important phenotypic differences among the three populations, CC-1690, ANC3 and ANC5 in response to nitrogen depletion treatment we used PCA to decompose the variation in the mass spectra. SC-MS values report differences in relative lipid and pigment composition of the single cells. PC1 refers to the absolute intensities of peaks in the mass spectra that cannot be assessed quantitatively using our MALDI-MS method (see Methods). PC2, however, separated between chlorophylls and DGTS while PC3 additionally separated between TAGs (**Figure 1**, for the PC loadings see Figure S9). Based on this analysis, we defined three phenotypes called 'high chlorophyll' (PC2 > 0 and PC3 < 5), 'high membrane lipid' (PC2 > 0 and PC3 <5) and 'high storage lipid' (PC3 > 5) (see Table S3). For exemplary spectra of the three phenotypes, see **Figure 2B**. For PC scores of the respective cells see Figure S10. The 'high chlorophyll' phenotype was ubiquitous in N-replete cultures and especially prominent on day 2 (e.g. 97.4 % of cells measured in N-replete CC-1690). Fisher's exact test showed that in deplete cultures there was no significant difference between the phenotype frequencies in CC-1690 and ANC3 on day 2 ($p=0.20$) while CC-1690 and ANC5 differed significantly ($p=0.008$). With increasing nitrogen limitation 'high chlorophyll' phenotypes made up a decreasing fraction of the population (see green circles in **Figure 2A**) while the fraction of 'high membrane lipid' phenotypes increases (**Table 1**). Focusing on the most abundant chlorophyll (chlorophyll a) and the most abundant extraplastidic membrane lipid in the spectra (DGTS (34:3)) a bivariate analysis revealed a marked transition between 'high chlorophyll' stages on day 2 and 'high membrane lipid' on day 9 in N-deplete cultures as can be seen in **Figure 3**. Remarkably, CC-1690 shows a distinct bimodal distribution including both spectra high in chlorophyll a and high in DGTS (34:3) on day 9.

The three populations also differed in the timing of the onset of the 'high storage lipid' phenotypes (**Table 1**) in N-depleted cultures (**Figure 1** and **Figure 2A**). In CC-1690 we detected 'high storage lipid' phenotypes throughout the time series (12.5 – 36.3 % of the cells in the population) while in ANC3, only small fractions of the populations showed 'high storage lipid' phenotype until day 6 (1.6% on day 2, 4.8% on day 6, see also Table S3). ANC5 showed a very small fraction of 'high storage lipid' phenotypes on day 4 (3.9%) and on day 6 (0.6%). Highest frequencies of 'high storage lipid' phenotypes for both isoclonal populations were found on day 9. ANC3 contained almost 40% of cells with a 'high storage lipid' phenotype while ANC5 contained the lowest level of 'high storage lipid' phenotype cells (14.8%) in comparison to the other two populations. Fisher's exact test showed that under deplete conditions, CC-1690 differed significantly both from ANC3 ($p = 0.00008$) and from ANC5 ($p \approx 0$) on day 9. In CC-1690, phenotype frequencies were not significantly different between day 6 and day 9 ($p=0.91$). CC-1690 was the first culture to respond to nitrogen stress with 'high storage lipid' phenotypes, but also the population that was able to retain the highest fraction of 'high chlorophyll' cells until day 9 (15.6 % in CC-1690, 3.6% ANC3 and 3.2% in ANC5). Furthermore, CC-1690 N-deplete and N-replete cultures displayed greater phenotypic similarity on day 9 than ANC3 and ANC5, as shown by the high overlap of contour plots of CC-1690 N-replete and N-deplete cultures in **Figure 1**.

Parallel chlorophyll measurements using microscopy

Since SC-MS only reports relative compound levels and we cannot assume one of the compounds to be present in equal amounts in all the single cells measured, we aimed to confirm the trends in chlorophyll levels that we observed using SC-MS using fluorescence microscopy. As per our MS data, the fluorescence microscopy showed that on day 2, the N-replete and N-deplete cultures tended to had comparable chlorophyll levels while on day 9

283 replete cultures were relatively much higher in chlorophyll than deplete cultures (**Figure 4**
284 and Supplementary information Table S4). Fluorescence microscopy also showed that ANC5
285 cells had relatively low absolute levels of chlorophyll on day 9. ANC3 still shows the highest
286 absolute chlorophyll intensities of all populations under N-deplete conditions on day 9
287 (**Figure 4** and Supplementary information Table S4).

288 ***Comparisons of pooled trait variation***

289 The TOP index is an estimate of the cumulative area of multidimensional trait space
290 that is covered by individuals of a population. We used bootstrapping to compare the
291 temporally pooled trait variation between isoclonal and diverse populations of equal size (100
292 cells). The analysis showed that the bootstrapped distribution of estimated trait variation
293 (TOP) for ANC3 was largely overlapping with that of CC1690, regardless of nitrogen
294 treatment (Figure S11a & b). By comparison, the distribution of ANC5 TOP index showed
295 lower levels of trait variation than CC1690 in both the deplete (mean difference = -180.79,
296 Figure S11c) and the replete (mean difference = -220.51, Figure S11d) environments.
297 However, in all cases the bootstrap probabilities that the clones had greater or lower
298 individual-level trait variation than the population were all <0.95 (reported in Figure S11),
299 and were therefore not statistically significant at the p=0.05 critical threshold.

300 We were interested first and foremost in the multidimensional trait variation of the
301 populations, but we also investigated differences in temporally pooled trait variance along
302 individual PC axes for each populations x nitrate treatment combination. ANC3 did not show
303 significant differences from CC1690 along PC2, but it showed significantly lower variance
304 than CC1690 in the replete environment, and significantly higher variance in the deplete
305 environment along PC3 (Table S5, Figure S11 & S12). By contrast, ANC5 showed lower
306 variance than CC1690 in all scenarios, except along PC2 in the deplete environment, where it

had significantly higher trait variance (Table S5, Figure S11 & S12).

Altogether, this suggests that both isoclonal populations had equal or lower phenotypic variation than the genetically diverse population in multidimensional trait space, but that they were able to display greater phenotypic variance in individual trait dimensions under nitrogen stress (Figure S11): ANC3 had greater variance along PC2 and ANC5 had greater variance along PC3 (Figure S12).

Discussion

The single-cell phenotype data collected here are the first of their kind in term of complexity and extent. The depth of information collected from each cell revealed marked cell-to-cell variation within each culture at each time point. At the population level, the measurements followed the general trends reported in the literature with regards to *C. reinhardti*'s responses to nitrogen depletion, including the decrease in chlorophyll, an increase in DGTS content, and the accumulation of TAGs (Yang et al., 2015, Park et al., 2015, Juergens et al., 2015). Following the phenotypic composition of the populations at the single-cell level over time renders a dynamic picture of changes in phenotypic variation within populations of *C. reinhardtii* in response to this well-studied nutrient stressor. Furthermore, it provides information about the amount of phenotypic variation generated by plasticity alone versus that generated by both plasticity and genetic diversity together.

Our results show that genetic diversity tends to result in greater multidimensional phenotypic variation among cells within a population over time during N-limitation than plasticity alone (**Figure 2A, Figure S11**). Phenotypic variation (i.e. the expression of all three phenotypes: 'high chlorophyll', 'high membrane lipid' and 'high storage lipid') in the genetically diverse population is maintained over the time course of the experiment, while the isoclonal populations show more synchronicity in their response to N-limitation. It has been reported that the accumulation of high levels of TAG are a mechanism to alleviate oxidative stress concurrent with the slowdown of anabolic metabolism upon N-limitation (Huner et al., 2012). We therefore attribute the 'high storage lipid' phenotype to cells that experience high N-limitation stress. While both isoclonal populations showed 'high storage lipid' phenotypes almost exclusively on day 9, the diverse population already showed cells with 'high storage lipid' phenotype within the first 6 days of the experiment. By contrast, CC-1690 also included

337 the highest fraction of cells with a 'high chlorophyll' phenotype on day 9. It should be noted
338 that the level of a certain metabolite or biopolymer (including chlorophyll) in a single cell is
339 the result both of its biosynthesis and degradation. Nevertheless, the presence of 'high
340 chlorophyll' cells on day 9 might be an indication of cells that are little affected by the
341 nitrogen-limitation, and is consistent with its relatively low nitrogen requirement (N*) and
342 high maximum specific growth rate (μ_{max} Figure S1 and S2). The functional interpretation of
343 the 'high membrane lipid' phenotype is more difficult because extraplastidic membranes are
344 involved in a variety of metabolic processes in the ER, the Golgi apparatus and the plasma
345 membrane (**Table 1**). Despite the clear change in DGTS/chlorophyll a ratio in N-deplete
346 cultures (**Figure 3**), the abundance of the 'high membrane lipid' phenotype and the variation
347 of DGTS/ chlorophyll a ratio in replete cultures suggests that the increase of 'high membrane
348 lipid' phenotypes is not only a response to nitrogen limitation, but is also part of the
349 phenotypic variation in the N-replete environment.

350 SC-MS suggested that ANC3 underwent a transition from 'high chlorophyll' to 'high
351 membrane lipid' phenotypes early on (70% 'high membrane lipid', 30% 'high chlorophyll' on
352 day 4). Fluorescence microscopy of the same population revealed that ANC3 still shows
353 highest chlorophyll levels on day 9 compared to CC-1690 and ANC5 (**Figure 4**, Table S4).
354 This suggests that downregulation of photosynthesis under N-limitation might be less
355 pronounced in ANC3. However, ANC3 also showed a relatively high fraction of 'high storage
356 lipid cells' on day 9, indicating high levels of nitrogen limitation. This is also in agreement
357 with the significantly higher nitrogen requirement (N*) of ANC3 compared to CC-1690
358 (Supporting Information, Figure S1). By contrast, ANC5 showed lowest chlorophyll values
359 per cell compared to both CC-1690 and ANC3 on day 9 in fluorescence microscopy.
360 However, the fewer 'high storage lipid' cells (14.8%) compared to both ANC3 and CC-1690

361 suggest an adaptive downregulation of photosynthesis. Population measures showed that
362 ANC5 has a significantly lower population-level growth rate, which further supports the
363 hypothesis that ANC5 shows conservative growth behavior beneficial in nutrient limited
364 environments. Based on these responses of the isoclonal populations, it would stand to reason
365 that they represent different strategies in coping with nutrient limitation. By keeping
366 photosynthetic activity low, ANC5 may decrease its risk of running into oxidative stress upon
367 intensification of nitrogen limitation. On the other hand, in keeping high amounts of
368 chlorophyll, ANC3 may be able to utilize available nitrogen more quickly when it is supplied
369 at a higher concentration in the environment (see **Figure 4** and Table S4). This is supported
370 by a faster maximal population growth rate (Figure S2), particularly in replete conditions
371 (Figure S2).

372 When we compared the full range of phenotypic variation across populations over
373 time, we found that the genetically diverse population tended to have an equal or greater
374 multidimensional phenotypic variation than the isoclonal populations, i.e. the cells more fully
375 covered the multidimensional trait space. This was despite the fact that the clones both
376 showed greater phenotypic variance along individual trait axes under N-limitation: ANC3
377 showed greater variance along PC3 and ANC5 along PC2. One explanation is that plasticity
378 in this system confers the ability to maintain high-fitness-associated phenotypes under stress
379 (i.e. N-limitation), providing phenotypic buffering, rather than promoting the expression of
380 phenotypic variance (Reusch, 2014). Accordingly, each clone is able to plastically buffer the
381 expression of low-fitness, highly stressed, phenotypes in one phenotypic dimension, but not
382 the other. By contrast, the genetically diverse population, which covers more of the
383 multidimensional phenotype space, may be phenotypically buffered to the influences of the
384 N-limitation along both individual phenotypic axes due to genetic compensation, or the

385 increase in the abundance of genotypes with high-fitness-associated phenotypes (Grether,
386 2005). This assumes that the reduced phenotypic variation along individual trait axes, but the
387 greater coverage of phenotypic space in multiple dimensions in the genetically diverse
388 population is adaptive. Though we did not measure the fitness of individual phenotypes, this
389 interpretation is supported by the relatively high population-level growth rate and low
390 nitrogen requirement of CC1690 compared to the isoclonal populations. Overall, our results
391 suggest that genetic diversity can produce equal or greater multidimensional phenotypic
392 variation (trait richness) under nitrogen stress as non-genetic sources, but that it can result in
393 significantly lower phenotypic variation in response to stress along individual phenotypic
394 dimensions.

395 Multidimensional phenotype data from single cells, such as those presented here, are
396 invaluable in the study of phenotypic adaptation. The key abilities of SC-MS are that (i)
397 multiple cellular processes can be monitored simultaneously, (ii) high-throughput analysis can
398 render a cross-section of the phenotypic composition of populations, and (iii) the method can
399 be applied on multiple time points in an experiment, which reveals information on changes in
400 the phenotypic composition of populations over time. Our experiments also show the benefit
401 and need for complementing single-cell mass spectrometric data with other phenotypic data
402 collected from the same population and the bridging of single-cell information with
403 population characteristics, which enhances this highly multiparametric experimental
404 approach. Future applications of the method should also aim to use the method in an
405 experimental context or include biological replicates for each measurement. The experiments
406 showed here further underline that SC-MS can detect biologically functional phenotypic
407 variation in populations, i.e. differences between cells that can make a difference for the
408 whole population. From this analysis, we learned that non-genetic multidimensional

409 phenotypic variation tends to be more limited and synchronous over time than genetically-
410 based phenotypic variation, but the cumulative non-genetic phenotypic variance over time can
411 be greater along individual phenotypic dimensions than that found in genetically diverse
412 populations. The consequences of these findings for eco-evolutionary dynamics are beyond
413 the scope of our study, but would be a fruitful avenue for future investigation.

Acknowledgements

We thank J. Sobek from the Functional Genomics Center Zürich for the help and expertise in the sample preparation for SC-MS, R. Steinhoff and Y. Suter for useful discussion and help with the data analysis. We thank M. Hertl for preparing microscopy samples and S. Flybjerg Norrelykke from ScopeM for his help with microscopy image processing. This manuscript was improved by the helpful comments of M. Czar, F. Pomati and F. Schreiber.

Figure 1 Contour plots of the PCA performed on the single-cell mass spectra. PC2 segregates between ‘high chlorophyll’ and ‘high membrane lipid’ cells corresponding to high and low PC2 values respectively. PC3 additionally segregates ‘high storage lipid’ cells. There is a general trend of all N-depleted populations from ‘high chlorophyll’ via ‘high membrane lipid’ towards ‘high storage lipid’.

Figure 2 A Schematic of the relative phenotypic composition of the populations over time. Each circle represents a 5% fraction of cells within the population (for more details see also Table S3). Green circles represent the ‘high chlorophyll’, blue circles the ‘high membrane lipid’ and red circles the ‘high storage lipid’ phenotypes. **B** Exemplary single cell mass spectra of the three phenotypes 'high chlorophyll', 'high membrane lipid' and 'high storage lipid'. The spectra were background subtracted using a proximate empty spot mass spectrum. ’High chlorophyll and ‘high membrane lipid’ cells are from replete ANC3 culture on day 9. ‘High storage lipid’ cell is from deplete ANC3 culture on day 9.

Figure 3 Violin plots of the log-transformed ratio of the peak area of DGTS (34:4) and chlorophyll a. Histograms are smoothed using a kernel density estimation. Red crossed indicate population averages. Replete ANC5 cultures on day 4 and day 6 showed too few successful measurements (less than 10) to be included in the analysis.

Figure 4 Chlorophyll fluorescence levels in relation to cell size determined using fluorescence microscopy.

Table 1 Functional assignment of compounds targeted by single-cell mass spectrometry and the reported population level responses in literature. The number of carbons and double bonds of lipids are indicated in parentheses, e.g. TAG (52:6). The detected TAG peaks can represent multiple isomers, e.g. TAG (18:0/18:2/16:4), TAG (18:0/18:4/16:2) and other isomers all contribute to the peak at TAG (52:6).

References

ACKERMANN, M. 2015. A functional perspective on phenotypic heterogeneity in microorganisms. *Nat Rev Microbiol,* 13**,** 497-508.

ALTSCHULER, S. J. & WU, L. F. 2010. Cellular heterogeneity: do differences make a difference? *Cell,* 141**,** 559-63.

AULD, J. R., AGRAWAL, A. A. & RELYEA, R. A. 2010. Re-evaluating the costs and limits of adaptive phenotypic plasticity. *Proceedings of the Royal Society B-Biological Sciences,* 277**,** 503-511.

BREKER, M., GYMREK, M. & SCHULDINER, M. 2013. A novel single-cell screening platform reveals proteome plasticity during yeast stress responses. *The Journal of Cell Biology,* 200**,** 839-850.

CARDILLO, G. 2007. *MyFisher23: a very compact routine for Fisher's exact test on 2x3 matrix* [Online]. Available: http://www.mathworks.com/matlabcentral/fileexchange/15399.

COLLINS, S. & GARDNER, A. 2009. Integrating physiological, ecological and evolutionary change: a Price equation approach. *Ecology letters,* 12**,** 744-57.

DEWITT, T. J., SIH, A. & WILSON, D. S. 1998. Costs and limits of phenotypic plasticity. *Trends in ecology & evolution,* 13**,** 77-81.

FONTANA, S., JOKELA, J. & POMATI, F. 2014. Opportunities and challenges in deriving phytoplankton diversity measures from individual trait-based data obtained by scanning flow-cytometry. *Frontiers in Microbiology,* 5.

FONTANA, S., PETCHEY, O. L. & POMATI, F. 2016. Individual-level trait diversity concepts and indices to comprehensively describe community change in multidimensional trait space. *Functional Ecology,* 30**,** 808-818.

FORSMAN, A. & WENNERSTEN, L. 2016. Inter-individual variation promotes ecological success of populations and species: evidence from experimental and comparative studies. *Ecography,* 39**,** 630-648.

GHALAMBOR, C. K., MCKAY, J. K., CARROLL, S. P. & REZNICK, D. N. 2007. Adaptive versus non-adaptive phenotypic plasticity and the potential for contemporary adaptation in new environments. *Functional Ecology,* 21**,** 394-407.

GIENAPP, P., TEPLITSKY, C., ALHO, J. S., MILLS, J. A. & MERILÄ, J. 2008. Climate change and evolution: disentangling environmental and genetic responses. *Molecular Ecology,* 17**,** 167-178.

GRETHER, G. F. 2005. Environmental change, phenotypic plasticity, and genetic compensation. *American Naturalist,* 166**,** E115-E123.

HAIRSTON, N. G., ELLNER, S. P., GEBER, M. A., YOSHIDA, T. & FOX, J. A. 2005. Rapid evolution and the convergence of ecological and evolutionary time. *Ecology letters,* 8**,** 1114-1127.

HENDRY, A. P. 2016. Key Questions on the Role of Phenotypic Plasticity in Eco-Evolutionary Dynamics. *Journal of Heredity,* 107**,** 25-41.

HUNER, N. P. A., BODE, R., DAHAL, K., HOLLIS, L., ROSSO, D., KROL, M., et al. 2012. Chloroplast redox imbalance governs phenotypic plasticity: the "grand design of photosynthesis" revisited. *Frontiers in Plant Science,* 3.

JUERGENS, M. T., DESHPANDE, R. R., LUCKER, B. F., PARK, J. J., WANG, H., GARGOURI, M., et al. 2015. The regulation of photosynthetic structure and function during nitrogen deprivation in Chlamydomonas reinhardtii. *Plant Physiology,* 167**,** 558-73.

KASHTAN, N., ROGGENSACK, S. E., RODRIGUE, S., THOMPSON, J. W., BILLER, S. J., COE, A., et al. 2014. Single-Cell Genomics Reveals Hundreds of Coexisting Subpopulations in Wild Prochlorococcus. *Science,* 344**,** 416-420.

KILHAM, S. S., KREEGER, D. A., LYNN, S. G., GOULDEN, C. E. & HERRERA, L. 1998. COMBO: a defined freshwater culture medium for algae and zooplankton. *Hydrobiologia,* 377**,** 147-159.

KLEIN, ALLON M., MAZUTIS, L., AKARTUNA, I., TALLAPRAGADA, N., VERES, A., LI, V., et al. 2015. Droplet Barcoding for Single-Cell Transcriptomics Applied to Embryonic Stem Cells. *Cell,* 161**,** 1187-1201.

KRISMER, J., SOBEK, J., STEINHOFF, R. F., FAGERER, S. R., PABST, M. & ZENOBI, R. 2015. Population Screening of Chlamydomonas reinhardtii with Single-Cell Resolution Using a High-throughput Micro Scale Sample Preparation for MALDI Mass-Spectrometry. *Appl Environ Microbiol*.

LU, S., ZONG, C., FAN, W., YANG, M., LI, J., CHAPMAN, A. R., et al. 2012. Probing meiotic recombination and aneuploidy of single sperm cells by whole-genome sequencing. *Science,* 338**,** 1627-30.

MACOSKO, EVAN Z., BASU, A., SATIJA, R., NEMESH, J., SHEKHAR, K., GOLDMAN, M., et al. 2015. Highly Parallel

Genome-wide Expression Profiling of Individual Cells Using Nanoliter Droplets. *Cell,* 161**,** 1202-1214.
MALCOM, J. W., HERNANDEZ, K. M., LIKOS, R., WAYNE, T., LEIBOLD, M. A. & JUENGER, T. E. 2015. Extensive cross-environment fitness variation lies along few axes of genetic variation in the model alga, Chlamydomonas reinhardtii. *New Phytologist,* 205**,** 841-851.
MERCHANT, S. S., PROCHNIK, S. E., VALLON, O., HARRIS, E. H., KARPOWICZ, S. J., WITMAN, G. B., et al. 2007. The Chlamydomonas genome reveals the evolution of key animal and plant functions. *Science,* 318**,** 245-50.
MILLER, R., WU, G. X., DESHPANDE, R. R., VIELER, A., GARTNER, K., LI, X. B., et al. 2010. Changes in Transcript Abundance in Chlamydomonas reinhardtii following Nitrogen Deprivation Predict Diversion of Metabolism. *Plant Physiology,* 154**,** 1737-1752.
PARK, J.-J., WANG, H., GARGOURI, M., DESHPANDE, R. R., SKEPPER, J. N., HOLGUIN, F. O., et al. 2015. The response of Chlamydomonas reinhardtii to nitrogen deprivation: a systems biology analysis. *The Plant Journal,* 81**,** 611-624.
PIGLIUCCI, M. 2005. Evolution of phenotypic plasticity: where are we going now? *Trends in ecology & evolution,* 20**,** 481-486.
REUSCH, T. B. H. 2014. Climate change in the oceans: evolutionary versus phenotypically plastic responses of marine animals and plants. *Evolutionary Applications,* 7**,** 104-122.
REYNOLDS, C. S. 2006. *Ecology of phytoplankton,* Cambridge, Cambridge University Press.
RINKE, C., SCHWIENTEK, P., SCZYRBA, A., IVANOVA, N. N., ANDERSON, I. J., CHENG, J.-F., et al. 2013. Insights into the phylogeny and coding potential of microbial dark matter. *Nature,* 499**,** 431-437.
SCHLICHTING, C. D. & PIGLIUCCI, M. 1998. *Phenotypic evolution: A reaction norm perspective*.
SCHREIBER, F., LITTMANN, S., LAVIK, G., ESCRIG, S., MEIBOM, A., KUYPERS, M. M. M., et al. 2016. Phenotypic heterogeneity driven by nutrient limitation promotes growth in fluctuating environments. *Nature Microbiology,* 1**,** 16055.
SCHUSTER, K. C., URLAUB, E. & GAPES, J. R. 2000. Single-cell analysis of bacteria by Raman microscopy: spectral information on the chemical composition of cells and on the heterogeneity in a culture. *Journal of Microbiological Methods,* 42**,** 29-38.
SIAUT, M., CUINÉ, S., CAGNON, C., FESSLER, B., NGUYEN, M., CARRIER, P., et al. 2011. Oil accumulation in the model green alga Chlamydomonas reinhardtii: characterization, variability between common laboratory strains and relationship with starch reserves. *BMC Biotechnology,* 11**,** 7-7.
SIMONS, A. M. 2011. Modes of response to environmental change and the elusive empirical evidence for bet hedging. *Proceedings of the Royal Society B-Biological Sciences,* 278**,** 1601-1609.
SPENCER, S. J., TAMMINEN, M. V., PREHEIM, S. P., GUO, M. T., BRIGGS, A. W., BRITO, I. L., et al. 2016. Massively parallel sequencing of single cells by epicPCR links functional genes with phylogenetic markers. *ISME J,* 10**,** 427-436.
SPITZER, MATTHEW H. & NOLAN, GARRY P. 2016. Mass Cytometry: Single Cells, Many Features. *Cell,* 165**,** 780-791.
WENNERSTEN, L. & FORSMAN, A. 2012. Population-level consequences of polymorphism, plasticity and randomized phenotype switching: a review of predictions. *Biological Reviews,* 87**,** 756-767.
WICKHAM, H. 2009. *ggplot2: Elegant Graphics for Data Analysis*, Springer-Verlag New York.
YAMAMICHI, M., YOSHIDA, T. & SASAKI, A. 2011. Comparing the Effects of Rapid Evolution and Phenotypic Plasticity on Predator-Prey Dynamics. *American Naturalist,* 178**,** 287-304.
YANG, D., SONG, D., KIND, T., MA, Y., HOEFKENS, J. & FIEHN, O. 2015. Lipidomic Analysis of <italic>Chlamydomonas reinhardtii</italic> under Nitrogen and Sulfur Deprivation. *PloS one,* 10**,** e0137948.
ZENOBI, R. 2013. Single-cell metabolomics: analytical and biological perspectives. *Science,* 342**,** 1243259.
ZONG, C., LU, S., CHAPMAN, A. R. & XIE, X. S. 2012. Genome-wide detection of single-nucleotide and copy-number variations of a single human cell. *Science,* 338**,** 1622-6.

Day 2
Day 4
Day 6
Day 9
CC-1690 N-deplete
CC-1690 N-replete
ANC3 N-deplete
ANC3 N-replete
ANC5 N-deplete
ANC5 N-replete
30
20
10
0
−10
−20
−50
0
50
Principle Component 3 (8.17 % variance explained)
Principle Component 2 (26 % variance explained)

A

Increasing N-limitation

Day 2 Day 4 Day 6 Day 9

CC-1690

ANC3

ANC5

high chlorophyll high membrane lipid high storage lipid

B

`high chlorophyll‘ cell

Chlorophylls

DGTS membrane lipids

r. int. (%)

90

60

30

0

`high membrane lipid‘ cell

DGTS membrane lipids

r. int. (%)

90

60

Chlorophyll

30

0

`high storage lipid‘ cell

r. int. (%)

90

60

Triacylglycerol lipids

30

0

m/z

750

780

810

840

870

900

930

Day 2 **Day 4** **Day 6** **Day 9**

log(DGTS/Chla)

-2 -1.5 -1 -0.5 0 0.5 1 1.5 2

CC-1690

N-deplete

N-replete

probability density

ANC3

N-deplete

N-replete

probability density

ANC5

N-deplete

N-replete

probability density

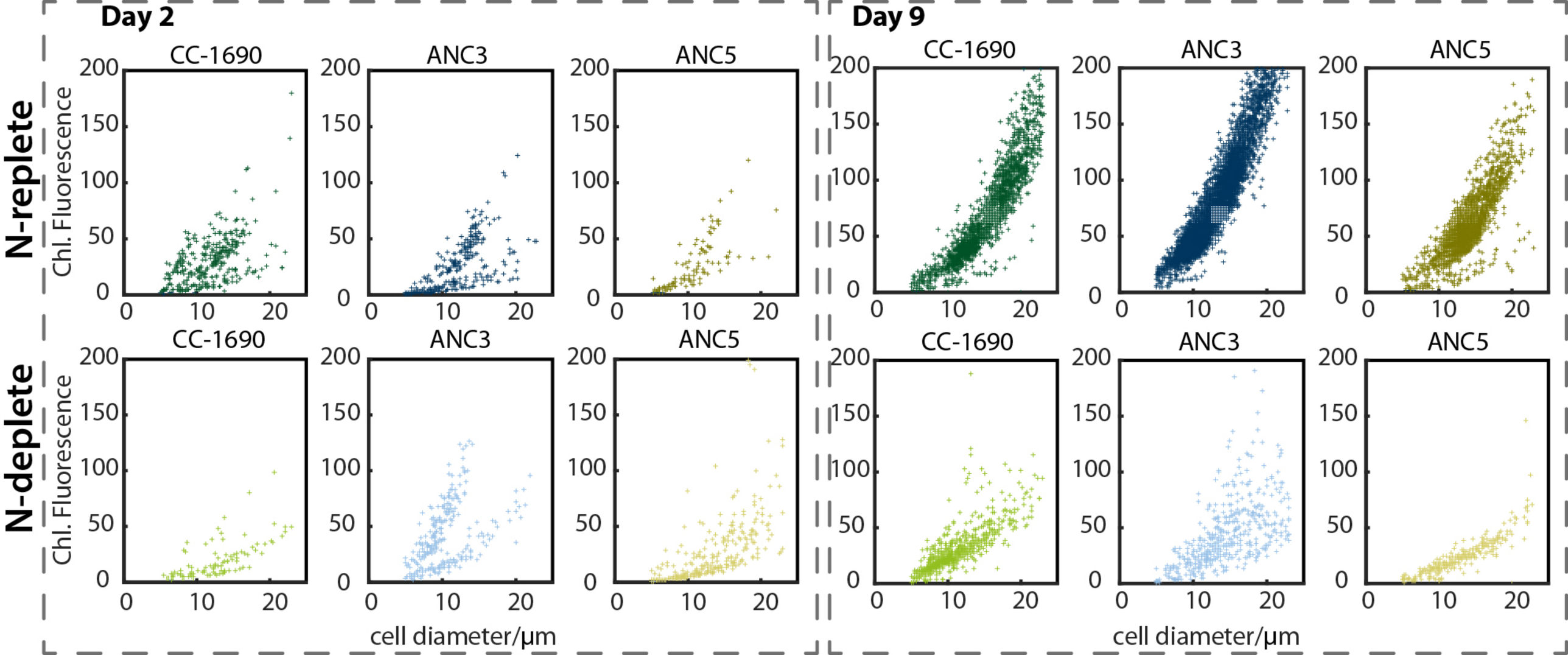
Day 2
Day 9
N-replete
N-deplete
CC-1690
ANC3
ANC5
Chl. Fluorescence
cell diameter/µm
0
50
100
150
200
0
10
20

Compound class and targeted peaks	Functional assignment
Photosynthetic pigments *Chlorophyll a, Chlorophyll b*	Light absorbance in photosynthetic complexes.
Thylakoid glycolipids *MGDG (34:7), DGDG (34:6), DGDG (34:5), DGDG (34:3), DGDG (34:2)*	Constituents of the thylakoid membrane embedding photosynthetic complexes.
Extraplastidic membrane lipids *DGTS (34:4), DGTS (34:3), DGTS (34:2), DGTS (36:7), DGTS (36:6), DGTS (36:5), DGTS (36:4)*	Extraplastidic membrane lipid that functionally replaces phosphatidylcholine. Present e.g. in endoplasmic reticulum, Golgi or mitochondria.
Neutral storage lipids *TAG (50:1), TAG (50:2), TAG (50:3), TAG (50:4), TAG (50:5), TAG (50:6), TAG (50:7), TAG (52:3), TAG (52:4), TAG (52:5), TAG (52:7),TAG (52:8)*	Energy storage in the form of reduced carbon. Accumulating in the form of lipid droplets in the cytoplasm.

Change under N-limitation
decrease (Juergens et al., 2015) (Miller et al., 2010)
decrease (Li et al., 2012) (Yoon et al., 2012)
increase (Yang et al., 2015)
increase (Liu et al., 2013) (Yang et al., 2015) (Boyle et al., 2012)